

Probing the Electronic Structures of Coordination Compounds by Transient Spectral Hole-Burning. Applications to Specifically Deuterated $[\text{Ru}(\text{bpy})_3]^{2+}$ Complexes

Hans Riesen* and Lynne Wallace

School of Chemistry, University College, The University of New South Wales,
Australian Defence Force Academy, Canberra, ACT 2600, Australia

Elmars Krausz

Research School of Chemistry, The Australian National University, Canberra, ACT 0200, Australia

Received May 22, 2000

Transient spectral hole-burning (THB), a powerful technique for probing the electronic structures of coordination compounds, is applied to the lowest excited $^3\text{MLCT}$ states of specifically deuterated $[\text{Ru}(\text{bpy})_3]^{2+}$ complexes doped into crystals of racemic $[\text{Zn}(\text{bpy})_3](\text{ClO}_4)_2$. Results are consistent with and complementary to conclusions reached from excitation-line-narrowing experiments. Two sets of $^3\text{MLCT}$ transitions are observed in conventional spectroscopy of $[\text{Ru}(\text{bpy}-d_n)_{3-x}(\text{bpy}-d_m)_x]^{2+}$ ($x = 1, 2; n = 0, 2; m = 2, 8; n \neq m$) complexes doped into $[\text{Zn}(\text{bpy})_3](\text{ClO}_4)_2$. The two sets coincide with the $^3\text{MLCT}$ transitions observed for the homoleptic $[\text{Ru}(\text{bpy}-d_m)_3]^{2+}$ and $[\text{Ru}(\text{bpy}-d_n)_3]^{2+}$ complexes and can thus be assigned to localized $^3\text{MLCT}$ transitions to the $\text{bpy}-d_m$ and $\text{bpy}-d_n$ ligands. The THB experiments presented in this paper exclude a two-site hypothesis. When spectral holes are burnt at 1.8 K into $^3\text{MLCT}$ transitions associated with the bpy and $\text{bpy}-d_2$ ligands in $[\text{Ru}(\text{bpy})(\text{bpy}-d_8)_2]^{2+}$, $[\text{Ru}(\text{bpy})_2(\text{bpy}-d_8)]^{2+}$, and $[\text{Ru}(\text{bpy}-d_2)_2(\text{bpy}-d_8)]^{2+}$, side holes appear in the $^3\text{MLCT}$ transitions associated with the $\text{bpy}-d_8$ ligands ≈ 40 and $\approx 30 \text{ cm}^{-1}$ higher in energy. Since energy transfer to sites 40 or 30 cm^{-1} higher in energy cannot occur at 1.8 K, the experiments unequivocally establish that the two sets of $^3\text{MLCT}$ transitions observed for $[\text{Ru}(\text{bpy}-d_n)_{3-x}(\text{bpy}-d_m)_x]^{2+}$ ($x = 1, 2$) complexes in $[\text{Zn}(\text{bpy})_3](\text{ClO}_4)_2$ occur on one molecular cation.

Introduction

We have shown by a wide range of experiments that the lowest three triplet metal-to-ligand charge-transfer ($^3\text{MLCT}$) zero-phonon lines (ZPLs), I–III, of $[\text{Ru}(\text{bpy})_3]^{2+}$ in crystalline $[\text{Zn}(\text{bpy})_3](\text{ClO}_4)_2$ are localized transitions on the electronic time scale.¹ If these $^3\text{MLCT}$ states were delocalized over all three ligands, a gradual shift of the three ZPLs as a function of the degree of deuteration would be observed. This is the case for $\pi-\pi^*$ transitions of aromatic organic molecules.² Other researchers have made the *incorrect* claim that this is also the case for deuteration of the $[\text{Ru}(\text{bpy})_3]^{2+}/[\text{Zn}(\text{bpy})_3](\text{ClO}_4)_2$ system.³ In fact, distinct transitions to the $\text{bpy}-d_n$ and $\text{bpy}-d_m$ ligand are observed in $[\text{Ru}(\text{bpy}-d_n)_{3-x}(\text{bpy}-d_m)_x]^{2+}$ ($x = 1, 2; n = 0, 2; m = 2, 8; n \neq m$) complexes in the $[\text{Zn}(\text{bpy})_3](\text{ClO}_4)_2$ host.^{4–7} For example, two sets of transitions are observed in $[\text{Ru}(\text{bpy})_{3-x}(\text{bpy}-d_2)_x]^{2+}$ ($x = 1, 2$)^{6,7} and the relative intensities of the two sets reflect the number of bpy and $\text{bpy}-d_2$ ligands (see Figure 2 in ref 6).

Usually, vibrational frequencies differ in the ground and excited states. Furthermore, excited-state vibrational frequencies are often *lower* than those in the ground state and will

consequently experience smaller deuteration shifts than corresponding vibrational frequencies in the ground state. Hence a shift of ZPLs to *higher* energy is usually seen upon deuteration, as the sum of zero-point energies of the vibrations in the ground state is lowered *more* than the corresponding sum for the excited state.

Figure 1 summarizes the energies of ZPLs of the lowest excited $^3\text{MLCT}$ states as observed in deuteration experiments. The energies were modeled using the two deuteration parameters Δ and Δ_{sp} . In localized $^3\text{MLCT}$ transitions, one ligand is directly involved and the other ligands act as spectators. Hence, there is a contribution to the deuteration shift by the ligand to which the charge transfer occurs and by the ligand or ligands that are spectators of the transition. We denote the contribution to the deuteration shift by the $\text{bpy}-d_8$ ligand to which the charge transfer occurs as Δ and the deuteration shift caused by a fully deuterated spectator ligand, $\text{bpy}-d_8$, which is indirectly involved in the transition, as Δ_{sp} . The spectator ligands see the metal center as Ru^{3+} in the excited state. The vibrational frequencies of the $[\text{Ru}(\text{bpy})_3]^{3+}$ complex are, on average, higher in energy than those of the $2+$ molecular cation.¹ Hence, Δ_{sp} can be expected to be negative. The main deuteration effect is due to the ligand to which the charge is transferred. For fractional deuteration ($\text{bpy}-d_n$, $\text{bpy}-d_m$), Δ and Δ_{sp} are multiplied by $n/8$ and $m/8$. For example

$$\Delta_{\text{bpy}-d_n} = \frac{n}{8}\Delta \quad \Delta_{\text{sp}}^{\text{bpy}-d_n} = \frac{n}{8}\Delta_{\text{sp}} \quad (1)$$

We emphasize here that this is only a first-order approximation. Different hydrogen positions on the bpy ligand may show slight

* Corresponding author. E-mail: h-riesen@adfa.edu.au. Fax: ++61-(0)2-6268-80-17.

- (1) Riesen, H.; Wallace, L.; Krausz, E. *Int. Rev. Phys. Chem.* **1997**, *16*, 291–359.
- (2) Broude, V. L.; Rashba, E. I.; Sheka, E. F. *Spectroscopy of Molecular Excitons*; Springer-Verlag: Berlin, 1985.
- (3) Yersin, H.; Humbs, W. *Inorg. Chem.* **1999**, *38*, 5820.
- (4) Riesen, H.; Krausz, E. *J. Chem. Phys.* **1993**, *99*, 7614.
- (5) Riesen, H.; Wallace, L.; Krausz, E. *J. Phys. Chem.* **1995**, *99*, 16807.
- (6) Riesen, H.; Wallace, L.; Krausz, E. *Inorg. Chem.* **1996**, *35*, 6908.
- (7) Riesen, H.; Wallace, L.; Krausz, E. *J. Phys. Chem.* **1996**, *100*, 17138.

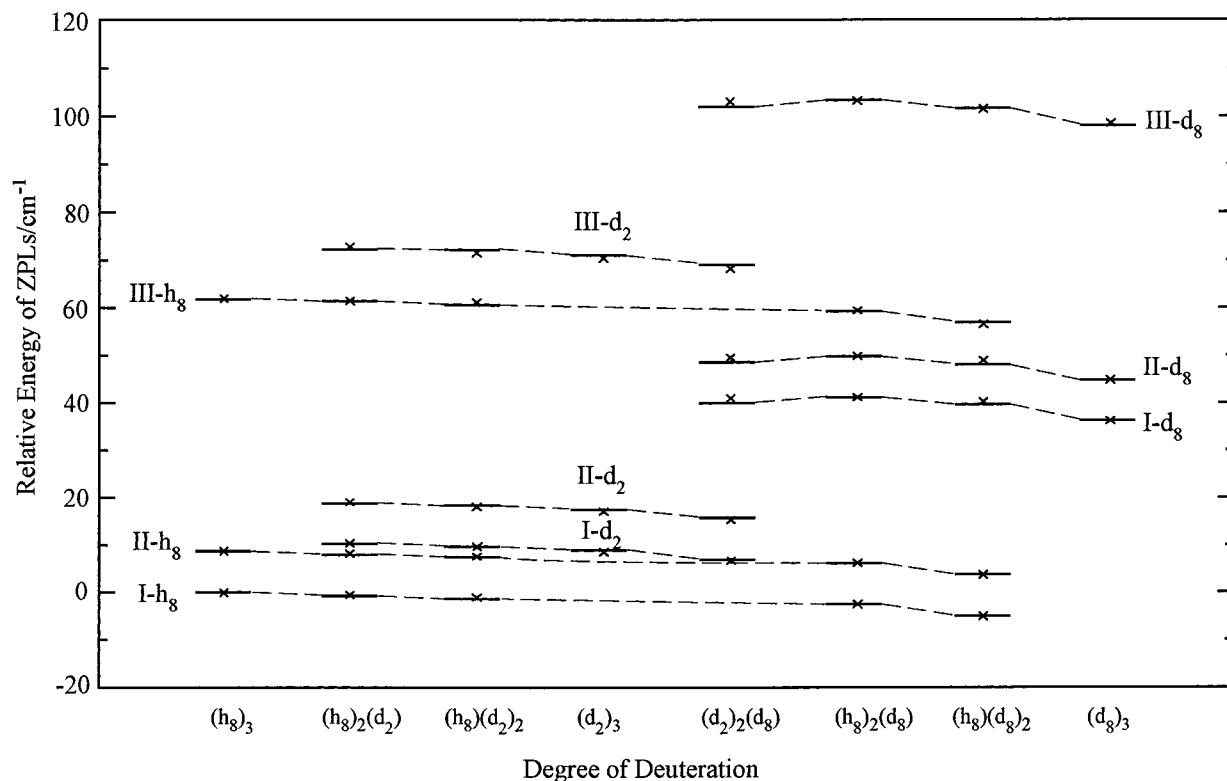


Figure 1. Summary of energy levels observed in [Ru(bpy- d_n)_{3-x}(bpy- d_m)_x]²⁺ complexes (abbreviated as (d_n)_{3-x}(d_m)_x; $d_0 = h_8$) doped into [Zn(bpy)₃](ClO₄)₂ (crosses) together with calculated levels (solid lines). For the calculation, $\Delta = 41 \text{ cm}^{-1}$ and $\Delta_{\text{sp}} = -2.5 \text{ cm}^{-1}$ were used. Energies are relative to transition I in [Ru(bpy)₃]²⁺/[Zn(bpy)₃](ClO₄)₂ at 17 685 cm⁻¹. Data were taken from refs 1, 4–7 and this work.

variations in the deuteration effect. The following additive scheme is used to calculate the energy shifts of the ³MLCT transitions I–III to the bpy- d_n and bpy- d_m ligands in the [Ru(bpy- d_n)_{3-x}(bpy- d_m)_x]²⁺/[Zn(bpy)₃](ClO₄)₂ series relative to transitions I–III of the [Ru(bpy)₃]²⁺/[Zn(bpy)₃](ClO₄)₂ system:

$$\Delta^{\text{bpy-}d_m} = \frac{m}{8}\Delta + (3-x)\frac{n}{8}\Delta_{\text{sp}} + (x-1)\frac{m}{8}\Delta_{\text{sp}} \quad (x = 1, 2, 3) \quad (2a)$$

$$\Delta^{\text{bpy-}d_n} = \frac{n}{8}\Delta + x\frac{m}{8}\Delta_{\text{sp}} + (2-x)\frac{n}{8}\Delta_{\text{sp}} \quad (x = 0, 1, 2) \quad (2b)$$

Quantitative agreement with experiment is achieved, as is illustrated in Figure 1, with $\Delta = 41 \text{ cm}^{-1}$ and $\Delta_{\text{sp}} = -2.5 \text{ cm}^{-1}$. The influence of the deuteration of a spectator ligand is over an order of magnitude smaller than that of the deuteration of the ligand directly involved in the metal-to-ligand charge-transfer process.

Racemic [Zn(bpy)₃](ClO₄)₂ and [Ru(bpy)₃](ClO₄)₂ crystallize in the same space group, *C*2/*c*.⁸ Bond angles and bond lengths are comparable for all three ligands, particularly in the ruthenium salt. However, one ligand is crystallographically unique and has an anion environment different from those of the two crystallographically equivalent ligands. This variation of the anion environment lifts the equivalence of the three ligands, and MLCT transitions to the unique ligand are calculated to be at higher energy by $\approx 900 \text{ cm}^{-1}$ by using a lattice sum based on a point charge model.⁸ The inequivalence of the ligands manifests itself in a pronounced dichroism in the metal–ligand plane (*a*–*b* plane) which is observable with a polarizing microscope or in polarized absorption spectra.⁸

Furthermore, the inequivalence of the two ligand positions can be directly observed in luminescence spectra of [Ru(bpy)₂–

(2,2′-bipyrazine)]²⁺ and [Ru(bpy)₂(3,3′-bipyridazine)]²⁺ doped into [Zn(bpy)₃](ClO₄)₂.^{9,10} Energy differences for the 2,2′-bipyrazine⁹ and the 3,3′-bipyridazine¹⁰ ligand, respectively. Thus, the lowest excited ³MLCT states in the [Ru(bpy)₃]²⁺/[Zn(bpy)₃](ClO₄)₂ system involve only the bpy ligands in the two crystallographically equivalent positions.

As a consequence, two sets of transitions are observed in the luminescence of [Ru(bpy- d_n)(bpy- d_m)₂]²⁺ complexes in the [Zn(bpy)₃](ClO₄)₂ host. This is because the bpy- d_n ligand can be either in a crystallographically equivalent position or in the unique position (see Figure 2). The former and latter configurations lead to ³MLCT emissions from the bpy- d_n and bpy- d_m ligands, respectively.^{1,4}

Another research group^{11,12} has invoked a multiple-site hypothesis to account for spectroscopic features of the [Ru(bpy- d_n)_{3-x}(bpy- d_m)_x]²⁺ complexes in the [Zn(bpy)₃](ClO₄)₂ host. However, systematic observations in selective deuteration experiments are entirely consistent^{1,4} with a localized description of the lowest excited ³MLCT levels and the *C*2/*c* crystal structure of the host. Transient-spectral hole-burning experiments are able to clearly discriminate between a single-site and a multiple-site system, as is elaborated in the following.

Electronic excitations of chromophores in the solid state are subject to inhomogeneous broadening. This arises from the variations in the local environments of individual chromophores. Often, laser techniques such as fluorescence line-narrowing (FLN), excitation line-narrowing (ELN), and spectral hole-

(9) Riesen, H.; Wallace, L.; Krausz, E. *J. Phys. Chem.* **1996**, *100*, 4390.

(10) Riesen, H.; Wallace, L.; Krausz, E. *Chem. Phys.* **1995**, *198*, 269.

(11) Yersin, H.; Humbs, W.; Strasser, J. In *Electronic and Vibronic Spectra of Transition Metal Complexes, Vol. II*; Yersin, H., Ed.; Topics in Current Chemistry 191; Springer-Verlag: Berlin, 1997; p 157.

(12) Huber, P.; Yersin, H. *J. Phys. Chem.* **1993**, *97*, 12705.

(8) Krausz, E.; Riesen, H.; Rae, A. D. *Aust. J. Chem.* **1995**, *48*, 929.

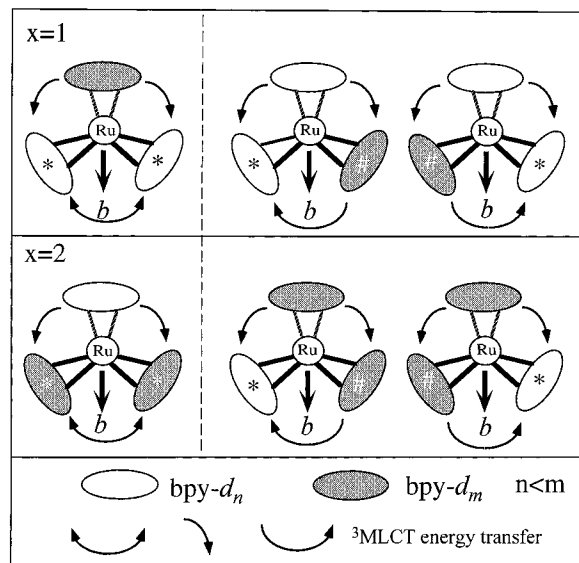


Figure 2. The two possible orientations with respect to the crystal axis b of $[\text{Ru}(\text{bpy}-d_n)_{3-x}(\text{bpy}-d_m)_x]^{2+}$ complexes with $x = 1, 2$ and $n < m$ in $[\text{Zn}(\text{bpy})_3](\text{ClO}_4)_2$. The $^3\text{MLCT}$ transitions to the ligand in the unique position on the b axis are several hundred wavenumbers higher in energy. As a consequence, the $x = 1$ system shows only $^3\text{MLCT}$ luminescence from the $\text{bpy}-d_n$ ligand at lowest temperature. In contrast, the $x = 2$ system also displays luminescence from the $\text{bpy}-d_m$ ligands at lowest temperatures when the $\text{bpy}-d_n$ ligand is in the unique position. Asterisks denote the ligands from which $^3\text{MLCT}$ luminescence occurs at lowest temperatures. Pound signs indicate ligands from which thermally activated luminescence may occur.

burning can overcome this broadening and it becomes possible to measure the finest details of an electronic structure.^{13–16}

In ELN, the luminescence of a subset of chromophores is selectively monitored and the wavelength of the laser is scanned in the region of interest, yielding a narrowed excitation spectrum (see Figure 3).

Spectral hole-burning can be classified as nonphotochemical, photochemical, or transient hole-burning (THB). In THB, a subset of chromophores within the inhomogeneously broadened transition is selectively excited by a pump laser. The modified absorption spectrum is measured by a probe laser. A depletion of the selected chromophores in the ground state can occur, leading to dips in the absorption spectrum.

ELN requires that the chromophore be luminescent. Thus, nonluminescent higher lying excited states in transition metal complexes can be investigated by *nonresonant* experiments only. In contrast, *resonant* THB experiments can be performed on any level as long as a measurable ground-state depletion is achieved.

Figure 3 compares the abilities of ELN and THB experiments to discriminate between a system consisting of a chromophore with two excited electronic levels, I and II, and a system with two crystallographic sites but with one electronic level only. In the first case, the two experiments provide the same results but, importantly, the THB experiment can also be performed *resonantly* on level II (not shown in Figure 3).

If a hole is burnt resonantly into level I, a nonresonant hole appears in level II. This nonresonant hole is broader because of relaxation effects but also because of the fact that energy levels may not be fully correlated, as is indicated in Figure 3.

In the two-site system of Figure 3b, the THB and the ELN experiments provide the same information if there is no energy transfer from site B to site A. Again, in the THB experiment, holes can be burnt resonantly into the higher energy site B. In this case, it is also possible to perform a resonant ELN experiment on site B if it is luminescent.

When there is very fast energy transfer from site B to site A, a steady-state ELN experiment provides parallel results for the two systems, as depicted in Figure 3. Further experiments such as time-resolved ELN are needed to discriminate between them. Time-resolved ELN experiments are applicable as long as the energy transfer from site B to site A is not too fast.

In contrast, the THB experiment discriminates clearly between the two cases, since, at low temperatures ($\Delta E \gg k_B T$; k_B is the Boltzmann constant), no hole will appear in the transition of site B when the pump laser wavelength lies within the inhomogeneously broadened transition of site A. This is because a subset of chromophores of site A is depleted and this subset is *independent* of site B. Energy transfer to a site higher in energy *cannot* occur when $\Delta E \gg k_B T$.

In the present paper, we demonstrate the effectiveness of THB in the detailed analysis of the two sets of ZPLs observed in $[\text{Ru}(\text{bpy}-d_n)_{3-x}(\text{bpy}-d_m)_x]^{2+}$ ($x = 1, 2$; $m \neq n$) systems.

Experimental Section

$\text{bpy}-6,6'-d_2$ and $\text{bpy}-d_8$ were prepared from bpy (Aldrich) as described in refs 7 and 17, respectively. $[\text{Zn}(\text{bpy})_3](\text{ClO}_4)_2$, $[\text{Ru}(\text{bpy})_{3-x}(\text{bpy}-d_8)_x]^{2+}$ ($x = 1, 2, 3$), and $[\text{Ru}(\text{bpy}-6,6'-d_2)_2(\text{bpy}-d_8)]^{2+}$ were prepared by standard literature methods.^{18–20}

Crystals of $[\text{Zn}(\text{bpy})_3](\text{ClO}_4)_2$ doped with the ruthenium complexes ($<0.1\%$ concentration) were grown by slow evaporation of aqueous solutions. The crystals displayed a *uniform* light yellow coloration.²¹

Luminescence and excitation spectra were obtained by using a Spectra Physics 375 dye laser pumped by a Spectra Physics 171 Ar^+ laser. The luminescence was dispersed by a Spex 1404 double monochromator and detected by an RCA 31034 photomultiplier. The signal was processed by a Stanford SRS 530 lock-in amplifier.

The SP 171 Ar^+ laser was used to pump both the SP 375 laser and a Coherent 599 dye laser in the transient-hole-burning measurements. The CR 599 dye laser served as the “pump” laser which created an excited-state population. The typical pump power was ≈ 8 mW. The SP 375 dye laser was used as the probe laser. The output of this laser was attenuated by neutral density filters and then stabilized by a Thorlabs CR200-A laser stabilizer. The intensity at the sample was ≈ 0.5 mW. The pump and probe beams were superimposed in a sample volume of $\approx 10^{-2}$ mm³.

The light of the probe and pump beams was modulated at 3.7 kHz and 79 Hz, respectively, by using New Focus model 3501 optical choppers. The intensity of the probe beam after the sample was measured by a silicon photodiode.

The signal was divided and processed by two SRS 510 lock-in amplifiers locked at 3.7 kHz and operating with 1 and 300 ms time constants, respectively. Hence, the lock-in amplifier with a time constant of 300 ms provided the average of the transmitted light intensities, $(I_{\text{on}} + I_{\text{off}})/2$, where I_{on} and I_{off} are the transmitted light intensities with the pump laser on and off, respectively. The output of the lock-in amplifier with the 1 ms time constant was fed into a third lock-in amplifier (SRS

(13) *Laser Spectroscopy of Solids*; Yen, W., Selzer, P. M., Eds.; Applied Physics 49; Springer-Verlag: Berlin, 1981.

(14) *Persistent Spectral Hole-Burning: Science and Applications*; Moerner, W. E., Ed.; Topics in Current Physics 44; Springer-Verlag: Heidelberg, Germany, 1988.

(15) Friedrich, J.; Haarer, D. *Angew. Chem., Int. Ed. Engl.* **1984**, *23*, 113.

(16) Krausz, E.; Riesen, H. *Laser Spectroscopy*. In *Inorganic Structure and Spectroscopy*; Solomon, E. I., Lever, A. B. P., Eds.; John Wiley: New York, 1999; Vol. I, Chapter 6.

(17) Fischer, G.; Puza, M. *Synthesis* **1973**, *4*, 218.

(18) Palmer, R. A.; Piper, T. S. *Inorg. Chem.* **1966**, *5*, 864.

(19) Sullivan, B. P.; Salmon, D. J.; Meyer, T. J. *Inorg. Chem.* **1978**, *17*, 3334.

(20) Crosby, G. A.; Elfring, W. H. *J. Phys. Chem.* **1976**, *80*, 2206.

(21) Riesen, H.; Krausz, E. *Chem. Phys. Lett.* **1998**, *287*, 388.

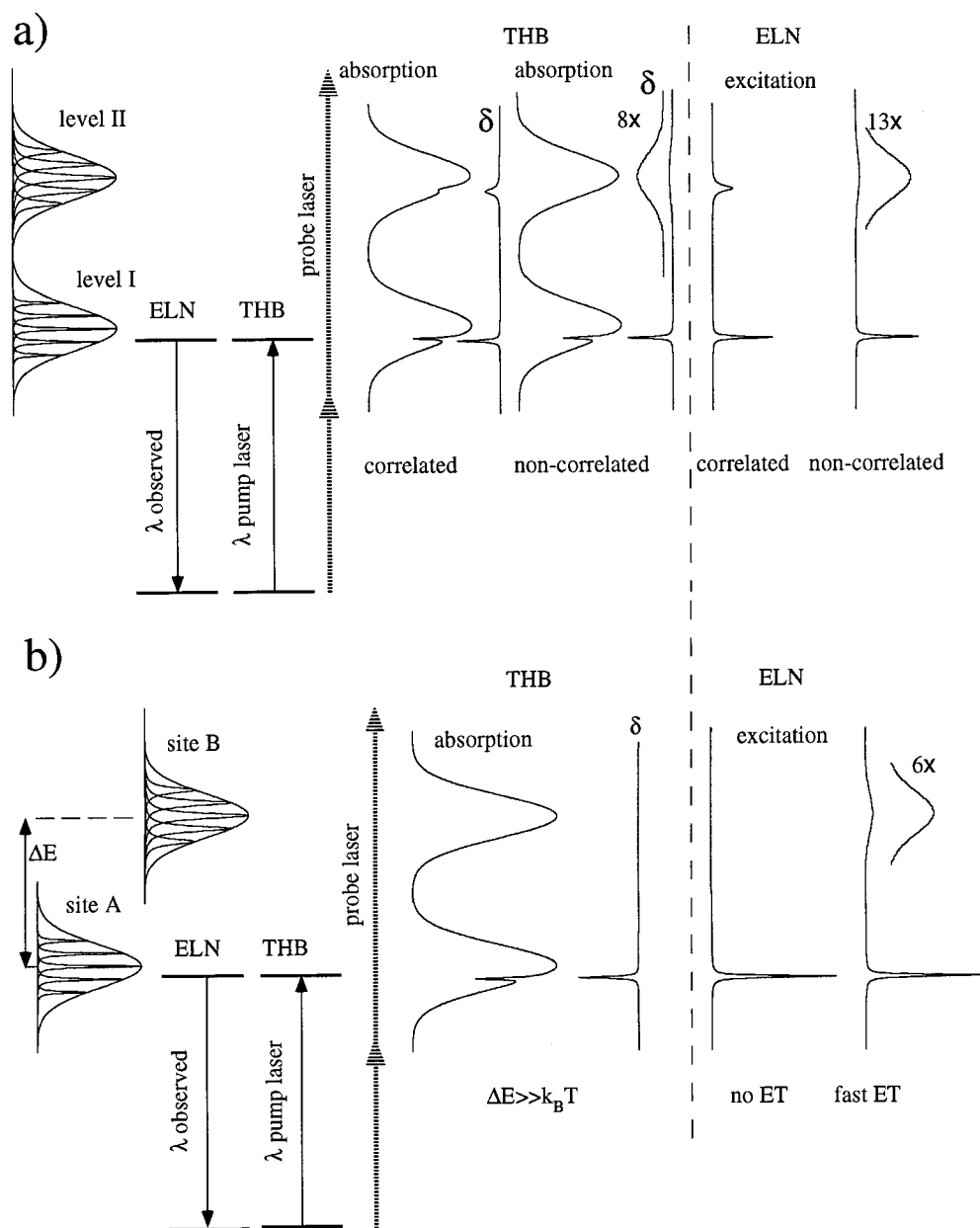


Figure 3. Schematic diagrams of THB and ELN in (a) a system consisting of two excited states and (b) a system with one excited state at two sites. THB and ELN spectra are shown for fully correlated and noncorrelated levels I and II in (a). For the case of two sites, system b, the ELN spectrum is shown for fast energy transfer from site B to site A and for no energy transfer. The trace δ shows the change in absorbance, ΔA , in the THB experiments.

510) with a reference frequency of 79 Hz. This third lock-in measured the change in transmitted light ($I_{\text{on}} - I_{\text{off}}$).

Figure 4 shows a schematic diagram of this very sensitive transient-spectral-hole-burning technique. The sensitivity of the present hole-burning technique is limited by dye laser intensity instabilities arising from fluctuations of the dye jet stream. We note here that the technique's sensitivity can be further enhanced by the application of Ti:sapphire and/or semiconductor lasers because of their superior light stabilities.

The signals $(I_{\text{on}} + I_{\text{off}})/2$ and $(I_{\text{on}} - I_{\text{off}})$ were acquired by a PC, providing I_{on} , I_{off} , and the change in optical density, $\Delta A = \log(I_{\text{off}}/I_{\text{on}})$. The wavelengths of the probe and pump beams were measured by a Burleigh WA-2000S jr wavemeter.

Results and Discussion

Excitation-Line-Narrowing Spectroscopy. Figure 5 compares the luminescence and excitation spectra of $[\text{Ru}(\text{bpy}-d_2)_2(\text{bpy}-d_8)]^{2+}$ and $[\text{Ru}(\text{bpy})_2(\text{bpy}-d_8)]^{2+}$ in crystals of $[\text{Zn}(\text{bpy})_3]$ -

$(\text{ClO}_4)_2$. The lower energy set of transitions shifts to higher energy upon the additional deuteration of bpy to $\text{bpy}-d_2$ whereas the transitions assigned to ${}^3\text{MLCT}$ excitations of the $\text{bpy}-d_8$ ligand shift slightly to lower energy by $2\Delta_{\text{sp}}/4$ as expected. As a consequence, the $\text{II}-d_8$ transition becomes more visible in the $[\text{Ru}(\text{bpy}-d_2)_2(\text{bpy}-d_8)]^{2+}$ spectrum as it becomes separated from the $\text{III}-d_2$ transition. Lowest temperature luminescence in the $[\text{Ru}(\text{bpy})_2(\text{bpy}-d_8)]^{2+}$ and $[\text{Ru}(\text{bpy}-d_2)_2(\text{bpy}-d_8)]^{2+}$ systems occurs only from the bpy or the $\text{bpy}-d_2$ ligands, respectively, since there is always one of the crystallographically equivalent ligand positions occupied by one of these ligands (see Figure 3).^{1,4} The $[\text{Ru}(\text{bpy}-d_2)_2(\text{bpy}-d_8)]^{2+}$ system allows the observation of ${}^3\text{MLCT}$ luminescence from the $\text{bpy}-d_8$ ligand at temperatures > 15 K (not illustrated here) since the energy gap is reduced by ≈ 10 cm^{-1} in comparison with that of the $[\text{Ru}(\text{bpy})_2(\text{bpy}-d_8)]^{2+}$ system. Energy levels obtained from these experiments are included in Figure 2.

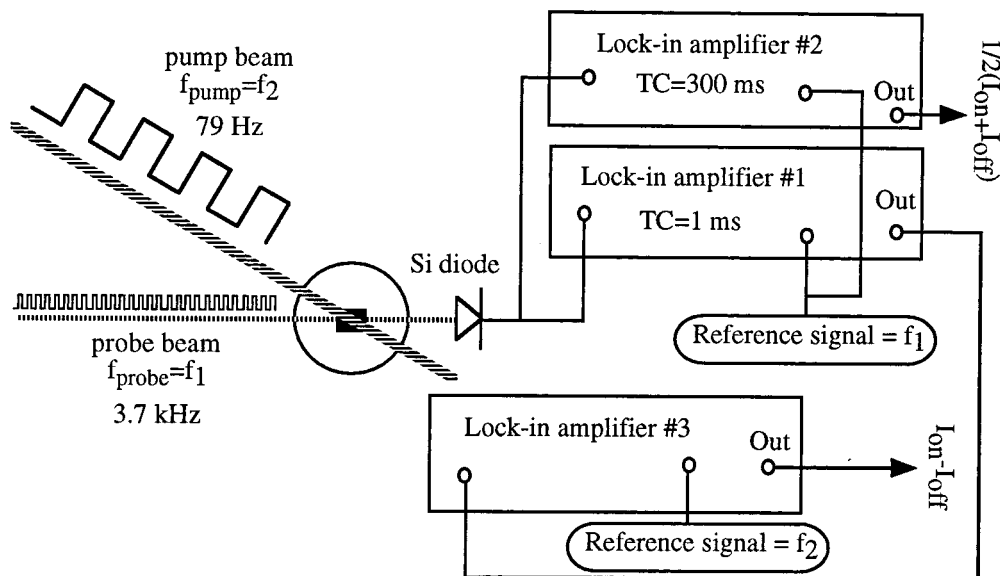


Figure 4. Setup for transient-spectral-hole-burning experiments. Coherent 599 and Spectra Physics 375 standing-wave dye lasers provided the pump and probe beams, respectively. Both lasers were pumped by a Spectra-Physics 171 Ar⁺ laser.

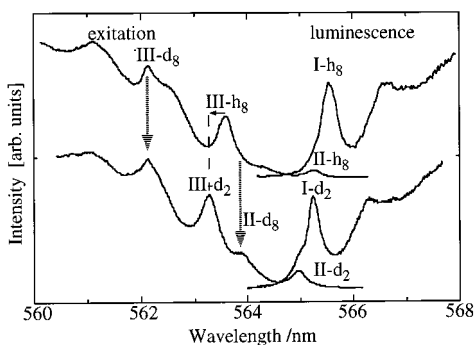


Figure 5. Nonselective excitation and luminescence spectra of $[\text{Ru}(\text{bpy})_2(\text{bpy}-d_8)]^{2+}$ and $[\text{Ru}(\text{bpy}-6,6'-d_2)(\text{bpy}-d_8)]^{2+}$ in $[\text{Zn}(\text{bpy})_3](\text{ClO}_4)_2$ at 1.8 K in the region of the electronic origins of the lowest excited ³MLCT states. The excitation spectra were recorded by scanning the dye laser while the luminescence was monitored at 570 nm and low resolution (≈ 1 nm) whereas the luminescence spectra were excited at 555 nm.

Figures 6 and 7 present narrowed excitation spectra for the $[\text{Ru}(\text{bpy})_2(\text{bpy}-d_8)]^{2+}/[\text{Zn}(\text{bpy})_3](\text{ClO}_4)_2$ and $[\text{Ru}(\text{bpy}-d_2)_2(\text{bpy}-d_8)]^{2+}/[\text{Zn}(\text{bpy})_3](\text{ClO}_4)_2$ systems. The monitoring wavelengths for the ³MLCT luminescence from the bpy and bpy-*d*₂ ligands, respectively, were varied systematically in these experiments. The same pattern of behavior was observed for both systems. In particular, the intensities of the ³MLCT transitions to the bpy-*d*₈ ligand decreased when the luminescence was observed at the lower energy side of the inhomogeneously broadened transition I-*h*₈ or I-*d*₂. We previously reported this effect for the $[\text{Ru}(\text{bpy})_2(\text{bpy}-d_8)]^{2+}/[\text{Zn}(\text{bpy})_3](\text{ClO}_4)_2$ system.⁴ It implies that the lower energy side of the inhomogeneous distribution of I-*h*₈ or I-*d*₂ is dominated by complexes that have the bpy-*d*₈ ligand in the crystallographically unique position (see Figure 3). ³MLCT transitions to ligands in this position are several hundred wavenumbers higher in energy and thus are not observed in the present spectra.

From the above observation we can conclude that the deuteration effects of spectator ligands, Δ_{sp} , are slightly different for the two crystallographic ligand positions. Consequently, Δ_{sp} is an average of $\Delta_{\text{sp}}^{\text{unique}}$ and $\Delta_{\text{sp}}^{\text{equivalent}}$. It follows that $|\Delta_{\text{sp}}^{\text{unique}}| > |\Delta_{\text{sp}}^{\text{equivalent}}|$.

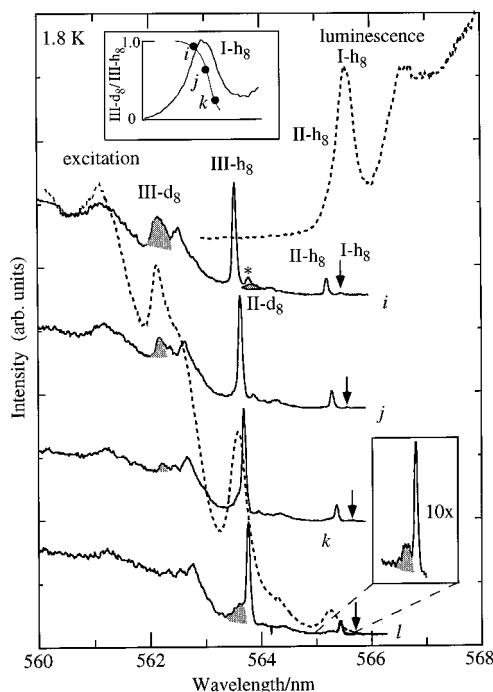


Figure 6. Narrowed excitation spectra of the $[\text{Ru}(\text{bpy})_2(\text{bpy}-d_8)]^{2+}/[\text{Zn}(\text{bpy})_3](\text{ClO}_4)_2$ system at 1.8 K. The nonselective excitation and luminescence spectra are shown as dashed lines. The wavelengths at which the luminescence was monitored with a bandwidth of 0.04 nm for the narrowed spectra are indicated by arrows. Origins due to transitions II-*d*₈ and III-*d*₈ are shaded. The lower inset shows the region of the II-*h*₈ transition. The upper inset shows the variation of the III-*d*₈/III-*h*₈ intensity ratio as a function of the monitoring wavelength. The asterisk denotes a peak which is caused by partially monitoring overlapping II-*h*₈ luminescence.

If the luminescence is monitored at the very red edge of the origin I, a broad feature appears at the higher energy sides of the transitions III-*h*₈, II-*h*₈, III-*d*₂, and II-*d*₂ in the excitation spectra. This feature is due to the second bpy-*h*₈ or bpy-*d*₂ ligand in the crystallographically equivalent position which after excitation transfers its ³MLCT energy to the crystallographically and chemically equivalent ligand from which ³MLCT luminescence occurs.^{1,4,21,22}

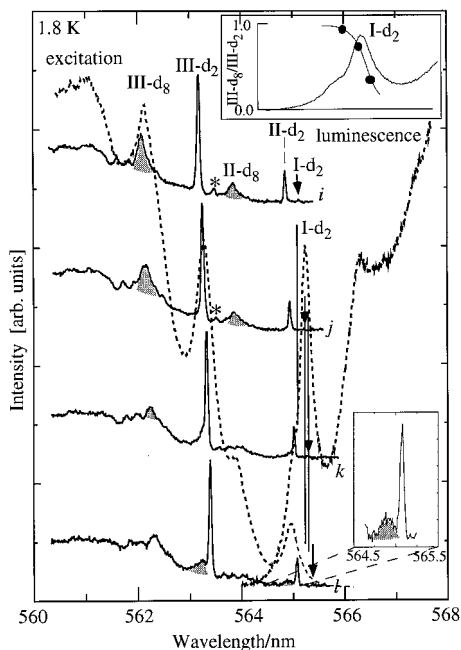


Figure 7. As in Figure 6 but for the $[\text{Ru}(\text{bpy}-6,6'\text{-d}_2)(\text{bpy}-\text{d}_8)]^{2+}/[\text{Zn}(\text{bpy})_3](\text{ClO}_4)_2$ system. The lower inset shows the region of the $\text{II}-\text{d}_2$ transition. The upper inset shows the variation of the $\text{III}-\text{d}_8/\text{III}-\text{d}_2$ intensity ratio as a function of the monitoring wavelength. Asterisks denote peaks which are caused by partially monitoring some $\text{II}-\text{d}_2$ luminescence.

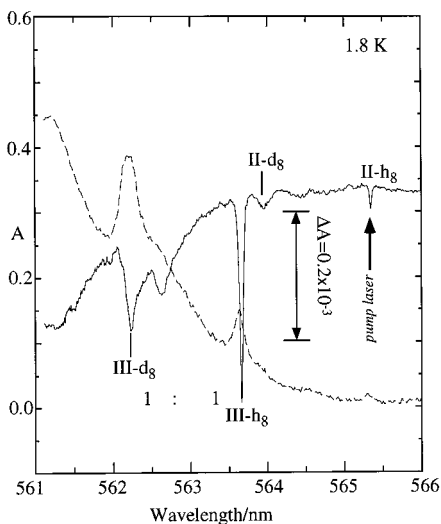


Figure 8. Transient spectral holes burnt into the ${}^3\text{MLCT}$ transitions of $[\text{Ru}(\text{bpy})(\text{bpy}-\text{d}_8)]^{2+}/[\text{Zn}(\text{bpy})_3](\text{ClO}_4)_2$ at 1.8 K (dashed line = absorbance A ; solid line = change in absorbance ΔA). The wavelength of the pump laser is indicated. The ratio of integrals of the hole areas for transitions $\text{III}-\text{h}_8$ and $\text{III}-\text{d}_8$ is indicated.

Yersin et al. have reported¹¹ a spectrum that is comparable to trace k in Figure 6. The existence of the transitions $\text{III}-\text{d}_8$ and $\text{II}-\text{d}_8$ and the broad feature was reported in our earlier work⁴ but was not noted in ref 11. We emphasize here that, in selective spectroscopy, it is essential to compare data with the nonselective spectrum. It is also necessary to consider the wavelength dependence of the selective spectra.

Transient-Spectral-Hole-Burning Experiments. (a) $\text{Ru}(\text{bpy})(\text{bpy}-\text{d}_8)]^{2+}$. Figure 8 displays transient spectral holes burnt into the spectrum of $[\text{Ru}(\text{bpy})(\text{bpy}-\text{d}_8)]^{2+}/[\text{Zn}(\text{bpy})_3](\text{ClO}_4)_2$. This system shows two sets of transitions which are

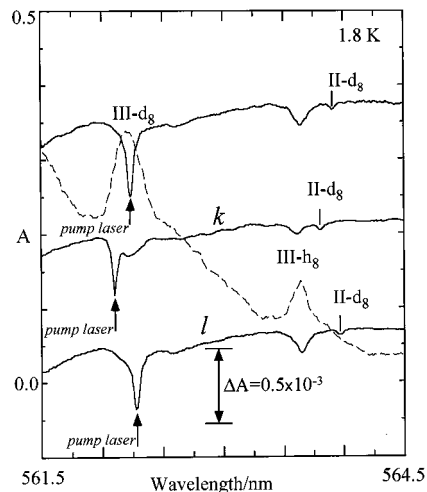


Figure 9. Transient spectral holes burnt into the ${}^3\text{MLCT}$ transitions of $[\text{Ru}(\text{bpy})(\text{bpy}-\text{d}_8)]^{2+}/[\text{Zn}(\text{bpy})_3](\text{ClO}_4)_2$ (dashed line = absorbance A ; solid lines = change in absorbance ΔA). The wavelength of the pump laser was varied within transition $\text{III}-\text{d}_8$ as indicated by arrows.

due to ${}^3\text{MLCT}$ excitations of the bpy and $\text{bpy}-\text{d}_8$ ligands.⁴ The experiment illustrated in Figure 8 establishes that the two sets of transitions observed in this system occur on *one molecular cation*, and the hypothesis of two or multiple sites^{11,12} can be excluded. If the two sets of transitions were due to two sites, no side holes would be observed at 1.8 K in the set of higher energy transitions. This is because energy transfer to a site $\approx 40 \text{ cm}^{-1}$ higher in energy is not possible at this temperature. The side holes observed in the $\text{II}-\text{d}_8$ and $\text{III}-\text{d}_8$ transitions upon burning into origin $\text{II}-\text{h}_8$ are broader because ${}^3\text{MLCT}$ energy levels of the $\text{bpy}-\text{d}_8$ and $\text{bpy}-\text{h}_8$ ligands are not well correlated.^{1,4}

The absorption spectrum in Figure 8 shows a $\text{III}-\text{h}_8/\text{III}-\text{d}_8$ intensity ratio of 1/2, reflecting the ratio of bpy and $\text{bpy}-\text{d}_8$ ligands. By burning a hole into the $\text{II}-\text{h}_8$ transition, we select molecular cations that have the bpy ligand in one of the two equivalent positions, excluding the configuration (see Figure 2) with the bpy ligand in the unique position. Every chromophore with a bpy ligand in one of the equivalent positions will have a $\text{bpy}-\text{d}_8$ ligand in the crystallographically equivalent position, leading to an intensity ratio of 1/1 for the transitions $\text{III}-\text{h}_8/\text{III}-\text{d}_8$ etc. This is indeed observed in the hole-burning spectrum of Figure 8.

The sensitivity of the present hole-burning technique is illustrated by the fact that the hole depth in Figure 8 is only $\approx 1\%$.

The resonant hole in $\text{II}-\text{h}_8$ in Figure 8 is instrumentally limited. A hole width of $\approx 0.001 \text{ cm}^{-1}$ was observed in Stark swept transient spectral-hole burning using a single-frequency laser.²³

Figure 9 shows spectra in which holes were burnt into origin $\text{III}-\text{d}_8$ at three different wavelengths in the region of transitions $\text{III}-\text{d}_8$, $\text{III}-\text{h}_8$ and $\text{II}-\text{d}_8$. Again side holes are observed in the $\text{III}-\text{h}_8$ and $\text{II}-\text{h}_8$ transitions (the latter is not shown in Figure 9). When the spectral hole is burnt into the high-energy side of the inhomogeneously broadened transition $\text{III}-\text{d}_8$, a broad side hole appears at slightly lower energy. This feature is due to the $\text{bpy}-\text{d}_8$ ligand in the crystallographically equivalent position. From the variation of the intensity ratio of the narrow feature to the broad feature and that of $\text{III}-\text{d}_8/\text{III}-\text{h}_8$, we conclude that the higher energy edge of the $\text{III}-\text{d}_8$ transition is dominated by complexes which have both deuterated ligands in the crystal-

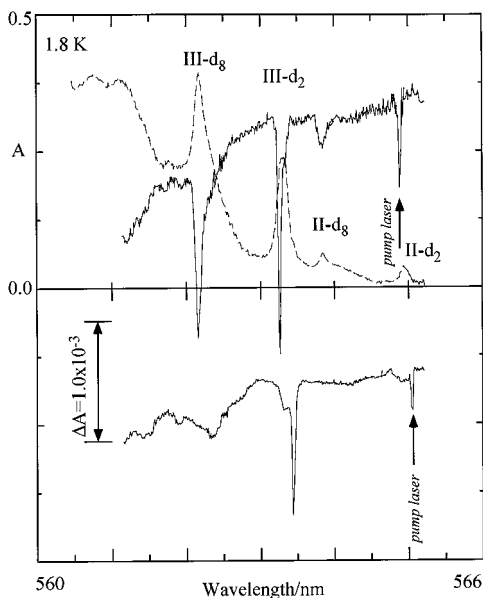


Figure 10. Transient spectral holes burnt into the $^3\text{MLCT}$ transitions of the $[\text{Ru}(\text{bpy}-6,6'\text{-d}_2)_2(\text{bpy}-\text{d}_8)]^{2+}/[\text{Zn}(\text{bpy})_3](\text{ClO}_4)_2$ system at 1.8 K for two wavelengths of the pump laser within the inhomogeneous profile of II-d_2 (dashed line = absorbance A ; solid lines = change in absorbance ΔA).

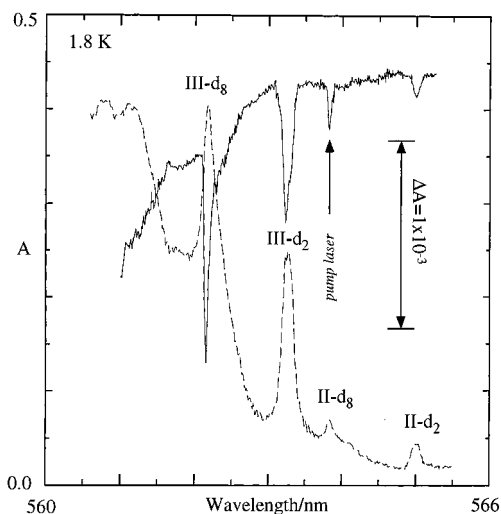


Figure 11. Transient spectral holes burnt into the $^3\text{MLCT}$ transitions of the $[\text{Ru}(\text{bpy}-6,6'\text{-d}_2)_2(\text{bpy}-\text{d}_8)]^{2+}/[\text{Zn}(\text{bpy})_3](\text{ClO}_4)_2$ system at 1.8 K for a wavelength of the pump laser within transition III-d_8 (dashed line = absorbance A ; solid line = change in absorbance ΔA).

lographically equivalent positions. This is in accord with observations in ELN experiments (see above and refs 1 and 4). As discussed above, this effect is accounted for by the slight variation in the contribution to the deuteration effect by the spectator ligand in the two crystallographic positions, $|\Delta\epsilon_{\text{sp}}^{\text{unique}}| > |\Delta\epsilon_{\text{sp}}^{\text{equivalent}}|$.

(b) $[\text{Ru}(\text{bpy})_2(\text{bpy}-\text{d}_8)]^{2+}$ and $[\text{Ru}(\text{bpy}-\text{d}_2)_2(\text{bpy}-\text{d}_8)]^{2+}$. Figures 10–13 illustrate THB experiments performed on the $[\text{Ru}(\text{bpy})_2(\text{bpy}-\text{d}_8)]^{2+}$ and $[\text{Ru}(\text{bpy}-\text{d}_2)_2(\text{bpy}-\text{d}_8)]^{2+}$ systems. Upon burning of holes into the $^3\text{MLCT}$ transitions II-h_8 and II-d_2 (see Figures 12 and 10), side holes appear in the $^3\text{MLCT}$ transitions involving the $\text{bpy}-\text{d}_8$ ligand. This clearly excludes a two-site hypothesis and again confirms that the two sets of transitions occur on *one molecular cation*. When pump laser wavelengths are chosen at the red edges of transitions II-h_8 and II-d_2 , the side holes in the transitions to $\text{bpy}-\text{d}_8$ vanish. This result is consistent with the observations in ELN spectroscopy (see

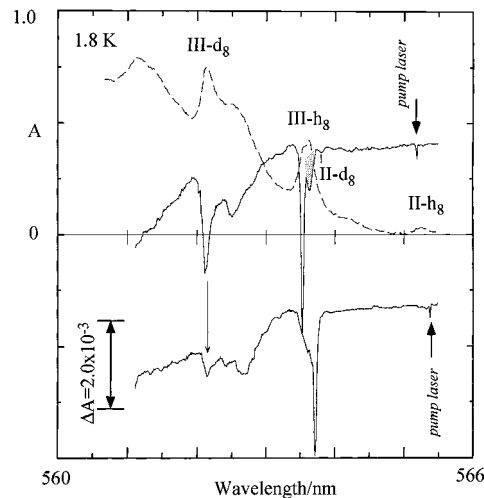


Figure 12. Transient spectral holes burnt into the $^3\text{MLCT}$ transitions of the $[\text{Ru}(\text{bpy})_2(\text{bpy}-\text{d}_8)]^{2+}/[\text{Zn}(\text{bpy})_3](\text{ClO}_4)_2$ system at 1.8 K for two wavelengths of the pump laser within the inhomogeneous profile of II-h_8 (dashed line = absorbance A ; solid lines = change in absorbance ΔA).

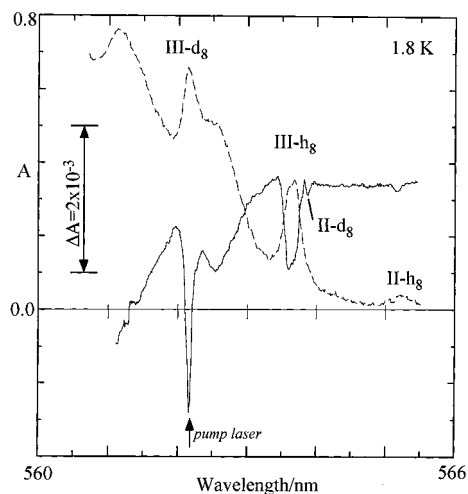


Figure 13. Transient spectral holes burnt into the $^3\text{MLCT}$ transitions of the $[\text{Ru}(\text{bpy})_2(\text{bpy}-\text{d}_8)]^{2+}/[\text{Zn}(\text{bpy})_3](\text{ClO}_4)_2$ system at 1.8 K for a wavelength of the pump laser within transition III-d_8 (dashed line = absorbance A ; solid line = change in absorbance ΔA).

Figures 6 and 7). Namely, the red edges of transitions II-h_8 and II-d_2 are dominated by complexes that have the $\text{bpy}-\text{d}_8$ ligand in the unique position. Transitions to the unique position are several hundred wavenumbers higher in energy and are thus not observable as holes in the II-d_8 and III-d_8 $^3\text{MLCT}$ transitions. When holes are burnt at the red edges, transitions involving the $\text{bpy}-\text{d}_2$ or bpy ligand are accompanied by broad side holes due to the $\text{bpy}-\text{d}_2$ or bpy ligand in the crystallographically equivalent position. This is also observed for a pump wavelength at the peak of transition II-h_8 , as is illustrated in the upper panel of Figure 12. This figure shows that the integrated hole area in the III-h_8 transition corresponds to the sum of integrated areas of the hole in the III-d_8 transition and the broad side hole in the III-h_8 transition. This is in accord with expectations, since the bpy ligand has either a $\text{bpy}-\text{d}_8$ or a bpy ligand in the crystallographically equivalent position. When the pump laser wavelength is chosen within the $^3\text{MLCT}$ transitions II-d_8 and III-d_8 in the $[\text{Ru}(\text{bpy}-\text{d}_2)_2(\text{bpy}-\text{d}_8)]^{2+}$ and $[\text{Ru}(\text{bpy})_2(\text{bpy}-\text{d}_8)]^{2+}$ systems, respectively (see Figures 11 and 13), side holes in the $^3\text{MLCT}$ transitions to the $\text{bpy}-\text{d}_2$ and $\text{bpy}-\text{h}_8$ ligands occur with intensity ratios of 1/1. This is because the crystallographically

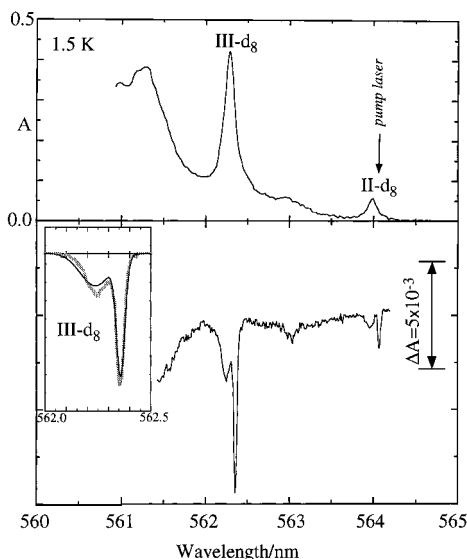


Figure 14. Results of transient spectral hole-burning for the $[\text{Ru}(\text{bpy}-d_8)_3]^{2+}/[\text{Zn}(\text{bpy})_3](\text{ClO}_4)_2$ system at 1.5 K for a wavelength of the pump laser at the red edge of origin $\text{II}-d_8$ (dashed line = absorbance A ; solid lines = change in absorbance ΔA). The inset shows the calculated line shape (solid line) in comparison with the experimental data for origin $\text{III}-d_8$.

equivalent positions are occupied by one $\text{bpy}-d_8$ ligand and a $\text{bpy}-d_2$ or bpy ligand. As a consequence, the holes in the transitions to the $\text{bpy}-d_8$ ligand are not accompanied by broad side holes. We note here that the variations observed for the III/II intensity ratios (Figures 10–13) are caused by the fact that III is predominantly polarized parallel to the crystal a^* axis whereas II is predominantly polarized parallel to the b axis.⁸ Hence the ratio depends on the way in which the crystals are mounted with respect to the polarization of the probe laser.

(c) $[\text{Ru}(\text{bpy}-d_8)_3]^{2+}$. A THB experiment in the $[\text{Ru}(\text{bpy}-d_8)_3]^{2+}/[\text{Zn}(\text{bpy})_3](\text{ClO}_4)_2$ system at 1.5 K is illustrated in Figure 14 for a pump laser wavelength at the red edge of the origin $\text{II}-d_8$. The resonant hole in $\text{II}-d_8$ and the nonresonant hole in $\text{III}-d_8$ are accompanied by broad side holes at higher energy.²¹ As discussed above, these features are due to the second $\text{bpy}-d_8$ ligand in the crystallographically equivalent positions. We note here that these side holes show the same ratio of integrated area to the narrower holes with pump laser wavelengths at the blue edge of transition $\text{II}-d_8$.²¹ If these holes were due to energy transfer within aggregated¹¹ complexes, the ratio would be strongly dependent on the pump laser wavelength. The separation between the narrow and the broad hole is $\approx 3 \text{ cm}^{-1}$ in the experiment illustrated in Figure 14. Hence, at 1.5 K, the ratio of the side hole area should only be $\approx e^{-3\text{cm}^{-1}/k_B(1.5\text{K})} = 0.056$ times the area observed in Figure 14. Thus we can again exclude that these side holes (or the broad side lines in ELN experiments) are due to energy transfer from other molecular cations. The inset shows that calculated and observed line shapes for the $\text{III}-d_8$ transition are in quantitative agreement. Line shapes were calculated using the procedure reported in ref 21.

(d) Intramolecular $^3\text{MLCT}$ Energy Transfer. We previously measured the intramolecular $^3\text{MLCT}$ energy-transfer rates between bpy or $\text{bpy}-d_8$ ligands in the crystallographically equivalent positions in the $[\text{Ru}(\text{bpy})_{3-x}(\text{bpy}-d_8)_x]^{2+}/[\text{Zn}(\text{bpy})_3](\text{ClO}_4)_2$ ($x = 0, 2$) systems by time-resolved luminescence-line-narrowing experiments.²² Using time-resolved luminescence spectroscopy, we were also able to estimate the rate of $^3\text{MLCT}$

Table 1. Intramolecular $^3\text{MLCT}$ Energy-Transfer Rates for $[\text{Ru}(\text{bpy}-d_n)_{3-x}(\text{bpy}-d_m)_x]^{2+}$ Complexes in $[\text{Zn}(\text{bpy})_3](\text{ClO}_4)_2$ at 1.8 K

| system | $^3\text{MLCT}$ energy-transfer process | $\Delta E/\text{cm}^{-1}$ | $k_{\text{ET}}/10^8 \text{ s}^{-1}$ | ref |
|--------|---|---------------------------|-------------------------------------|-----------------|
| 0 8 2 | $\text{bpy}-d_8 \rightarrow \text{bpy}-d_8$ | 3.5 ± 0.5 | 1.2 ± 0.2 | 22 ^b |
| 0 0 0 | $\text{bpy} \rightarrow \text{bpy}$ | 3.5 ± 0.5 | 1.3 ± 0.2 | 22 ^b |
| 0 2 2 | $\text{bpy}-d_2 \rightarrow \text{bpy}$ | 10 ± 1 | 21 ± 8 | 7 |
| 2 8 1 | $\text{bpy}-d_8 \rightarrow \text{bpy}-d_2$ | 34 ± 1 | 420 ± 50 | this work |
| 0 8 2 | $\text{bpy}-d_8 \rightarrow \text{bpy}$ | 45 ± 1 | 850 ± 50 | this work |

^a To calculate k_{ET} , we assumed that $k_{\text{BT}}/k_{\text{ET}} = e^{-\Delta E/k_B T}$. ^b This reference reports the sum of transfer and back-transfer rates, $k_{\text{ET}} + k_{\text{BT}}$.

energy transfer from the $\text{bpy}-d_2$ ligand to the bpy ligand in the crystallographically equivalent positions in the $[\text{Ru}(\text{bpy})(\text{bpy}-d_2)_2]^{2+}/[\text{Zn}(\text{bpy})_3](\text{ClO}_4)_2$ system.⁷ Results of these experiments are summarized in Table 1.

THB experiments can provide information regarding the homogeneous line width of higher lying excited ZPLs. This information is not accessible by (nonresonant) ELN experiments because energy levels are seldom fully correlated. Figures 9 and 11 provide new results regarding the intramolecular $^3\text{MLCT}$ transfer rates in specifically deuterated $[\text{Ru}(\text{bpy})_3]^{2+}$ complexes.

When the pump laser is at the high-energy edge of transition $\text{III}-d_8$ in the $[\text{Ru}(\text{bpy})(\text{bpy}-d_8)_2]^{2+}/[\text{Zn}(\text{bpy})_3](\text{ClO}_4)_2$ system, complexes with both $\text{bpy}-d_8$ ligands in the crystallographically equivalent positions are predominantly excited (trace k in Figure 9). In contrast, when the pump laser is at the red edge of transition $\text{III}-d_8$, complexes with one $\text{bpy}-d_8$ ligand in the unique position are predominantly selected (trace l in Figure 9). Resonant hole widths of 1.2 and 2.1 cm^{-1} are observed in the former and latter experiments, respectively. When both $\text{bpy}-d_8$ ligands are in the crystallographically equivalent positions, no energy transfer to a bpy ligand is possible. In contrast, when the bpy ligand is in one of the crystallographically equivalent positions, $^3\text{MLCT}$ energy transfer from $\text{bpy}-d_8$ to bpy may occur. Hence, the increase in hole width reflects the rate of $^3\text{MLCT}$ energy transfer from $\text{bpy}-d_8$ to bpy .

This transfer rate can be quantified by approximating the hole width Γ_{hole} with

$$\Gamma_{\text{hole}} \approx 2\Gamma_{\text{h}} + \Gamma_{\text{instrumental}} \quad (3)$$

where Γ_{h} is the homogeneous line width given by

$$\Gamma_{\text{h}} = \frac{1}{2\pi T_1} \quad (4)$$

T_1 is the effective lifetime of level $\text{III}-d_8$ at 1.8 K. Dephasing processes (T_2) can be neglected since the direct relaxation rates dominate.

In the first case (trace k in Figure 9), the homogeneous line width Γ_{h} is determined by the rate of intraligand relaxation from level III to level II , $k_{\text{III} \rightarrow \text{II}}$, in the excited $\text{bpy}-d_8$ ligand and by the rate of intramolecular energy transfer to the chemically and crystallographically equivalent $\text{bpy}-d_8$ ligand. The contribution to the hole width by the latter rate can be neglected because its rate of $\approx 10^8 \text{ s}^{-1}$ corresponds to a broadening by 15 MHz only. Using the instrumental line width $\Gamma_{\text{instrumental}}$ of 0.9 cm^{-1} (27 GHz) in eq 3 and applying eq 4, we can calculate a $\text{III} \rightarrow \text{II}$ relaxation rate of $k_{\text{III} \rightarrow \text{II}} = 2.8 \times 10^{10} \text{ s}^{-1}$ from the resonant hole width observed in trace k of Figure 9.

In the second case (trace l in Figure 9), energy transfer from the $\text{bpy}-d_8$ ligand to the bpy ligand occurs. Hence the effective

lifetime T_1 of level III- d_8 is given by

$$1/T_1 = k_{\text{III} \rightarrow \text{II}} + k_{\text{ET}} \quad (5)$$

where k_{ET} is the rate of $^3\text{MLCT}$ energy transfer from the bpy- d_8 ligand to the bpy ligand. Using the resonant hole width in trace 1 of Figure 9, we obtain $k_{\text{ET}} = 8.5 \times 10^{10} \text{ s}^{-1}$.

The resonant hole width in Figure 11 can be used to calculate the rate of $^3\text{MLCT}$ energy transfer from the bpy- d_8 ligand to the bpy- d_2 ligand in the crystallographically equivalent positions. In this case, the only significant broadening mechanism is due to the energy transfer since the intraligand $\text{II} \rightarrow \text{I}$ relaxation rate is very slow ($3.7 \times 10^6 \text{ s}^{-1}$).²²

The resonant hole width in II- d_8 is 1.35 cm^{-1} in Figure 11. This is a significant increase over the instrumentally limited resonant hole width of 0.9 cm^{-1} observed in Figure 10. (The II- d_2 hole width in Figure 10 shows the instrumental resolution only and is $\approx 30 \text{ MHz}$ when measured at highest resolution.²³) Using eqs 3 and 4, we can then calculate the rate of $^3\text{MLCT}$ energy transfer from the bpy- d_8 ligand to the bpy- d_2 ligand in the crystallographically equivalent position as $k_{\text{ET}} = 4.2 \times 10^{10} \text{ s}^{-1}$.

The $^3\text{MLCT}$ intramolecular energy transfer rates in Table 1 show a power dependence on the energy gap ΔE of 2.52 ± 0.03 :

$$k_{\text{ET}} \propto \Delta E^{2.52 \pm 0.03} \quad (6)$$

Intramolecular relaxation rates based on the direct process are dependent on the density of phonon states.¹³ Not surprisingly, the result in eq 6 deviates from the cubic dependence of the

density of phonon states in the Debye approximation. It is clear that the Debye approximation is inadequate, particularly in the case of a molecular crystal.

Conclusions

We have demonstrated that THB can be a highly effective probe in determining the electronic structure of coordination compounds. Our experimental setup allows for the detection of very shallow spectral holes ($< 0.01\%$). The present work confirms unequivocally that the two sets of transitions observed in $[\text{Ru}(\text{bpy}-d_n)_{3-x}(\text{bpy}-d_m)_x]^{2+}$ ($m \neq n$; $x = 1, 2$) complexes occur on one molecular cation only and a multiple-site hypothesis proposed in refs 11 and 12 can be excluded. These observations, together with a wide range of other experiments, such as Zeeman and Stark measurements, clearly establish that the lowest excited $^3\text{MLCT}$ states in $[\text{Ru}(\text{bpy})_3]^{2+}$ are localized. This phenomenology is put in a broader context by our comprehensive review¹ of the spectroscopic properties of ruthenium(II) and osmium(II) diimine complexes. In osmium(II) complexes, varying degrees of delocalized $^3\text{MLCT}$ behavior can occur.

The spectra observed for specifically deuterated ruthenium(II) complexes (see Figure 2) have been rationalized on the basis of a $C2/c$ crystal structure and a model parametrizing the deuteration effects of participating and spectator ligands on the localized $^3\text{MLCT}$ ZPLs. Furthermore, valuable direct measurements of the dependence of intramolecular $^3\text{MLCT}$ energy transfer rates on the energy gap have been made and interpreted.

IC0005386